Published in final edited form as:
J Control Release. 2012 January 30; 157(2): 249–259. doi:10.1016/j.jconrel.2011.09.074.

Addition of Ascorbic Acid to the Extracellular Environment Activates Lipoplexes of a Ferrocenyl Lipid and Promotes Cell Transfection

Burcu S. Aytar[a], **John P. E. Muller**[a], **Sharon Golan**[b], **Shinichi Hata**[c], **Hiro Takahashi**[c], **Yukishige Kondo**[c], **Yeshayahu Talmon**[b,*], **Nicholas L. Abbott**[a,*], and **David M. Lynn**[a,*]

[a]Department of Chemical and Biological Engineering, University of Wisconsin - Madison, 1415 Engineering Drive, Madison, Wisconsin 53706

[b]Department of Chemical Engineering, Technion-Israel Institute of Technology, Haifa 32000, Israel

[c]Dept. of Industrial Chemistry, Tokyo University of Science, Tokyo, Japan

Abstract

The level of cell transfection mediated by lipoplexes formed using the ferrocenyl lipid bis(11-ferrocenylundecyl)dimethylammonium bromide (BFDMA) depends strongly on the oxidation state of the two ferrocenyl groups of the lipid (reduced BFDMA generally mediates high levels of transfection, but oxidized BFDMA mediates very low levels of transfection). Here, we report that it is possible to chemically transform inactive lipoplexes (formed using oxidized BFMDA) to "active" lipoplexes that mediate high levels of transfection by treatment with the small-molecule reducing agent ascorbic acid (vitamin C). Our results demonstrate that this transformation can be conducted in cell culture media and in the presence of cells by addition of ascorbic acid to lipoplex-containing media in which cells are growing. Treatment of lipoplexes of oxidized BFDMA with ascorbic acid resulted in lipoplexes composed of reduced BFDMA, as characterized by UV/vis spectrophotometry, and lead to activated lipoplexes that mediated high levels of transgene expression in the COS-7, HEK 293T/17, HeLa, and NIH 3T3 cell lines. Characterization of internalization of DNA by confocal microscopy and measurements of the zeta potentials of lipoplexes suggested that these large differences in cell transfection result from (i) differences in the extents to which these lipoplexes are internalized by cells and (ii) changes in the oxidation state of BFDMA that occur in the extracellular environment (i.e., prior to internalization of lipoplexes by cells). Characterization of lipoplexes by small-angle neutron scattering (SANS) and by cryogenic transmission electron microscopy (cryo-TEM) revealed changes in the nanostructures of lipoplexes upon the addition of ascorbic acid, from aggregates that were generally amorphous, to aggregates with a more extensive multilamellar nanostructure. The results of this study provide guidance for the design of redox-active lipids that could lead to methods that enable spatial and/or temporal control of cell transfection.

*Corresponding Authors: Yeshayahu Talmon, ishi@tx.technion.ac.il.; Nicholas L. Abbott, Tel: (608) 265-5278; abbott@engr.wisc.edu; David M. Lynn, Tel: (608) 262-1086; dlynn@engr.wisc.edu.

Supplementary Data. Supplementary data to this article can be found online at doi:

Keywords

Ferrocenyl lipid; lipoplexes; transfection; nanostructure; ascorbic acid; external stimulus

Introduction

Cationic lipids have been investigated broadly as non-viral agents for the delivery of DNA to cells [1–6]. Early studies demonstrated that significant levels of cell transfection could be achieved by formulating cationic lipid/DNA complexes (lipoplexes) using lipids with relatively simple molecular structures (e.g., a simple cationic head group and several hydrophobic tails) [7, 8]. Over time, however, the structures and properties of lipids used for cell transfection have evolved to include chemical functionality designed to overcome or address a variety of intracellular barriers that limit cell transfection efficiency. For example, lipids have been designed to form lipoplexes that are stable in complex extracellular environments (including in the presence of serum proteins) [9–11] and/or release their cargo (DNA) in response to intracellular stimuli, including the presence of reducing agents [12–16] (e.g., glutathione), changes in pH [15, 17–19], or the presence of specific enzymes [20, 21]. The design of lipids that promote more efficient intracellular trafficking of internalized DNA has contributed significantly to the development of lipoplex-based approaches to DNA delivery.

In contrast to efforts to design functional lipids that promote the intracellular trafficking of DNA, relatively few studies have reported on the design of lipids that can be transformed (or "activated" toward transfection) in response to externally–controlled stimuli applied in *extracellular* environments (e.g., so as to influence extents to which complexes are either internalized or not internalized by cells) [22–24]. This latter approach could provide lipoplexes that enable control over the timing of the delivery of DNA to cells (i.e., "temporal control" of transfection) or, alternatively, allow delivery of DNA to sub-populations of cells within a larger population (i.e., "spatial control" of transfection by spatially-controlled delivery of an activating agent). The design of lipids that offer the ability to achieve external control over the timing and the locations at which DNA is available to cells could potentially find use in a broad range of applications, ranging from basic biomedical research (e.g., the design of transfected cell arrays) [25–29], engineering of tissues with complex tissue architectures [30–33], and, potentially, for the development of new gene-based therapies. In this current study, we report a step toward the realization of general and facile principles for spatial and temporal control over the lipoplex-mediated delivery of DNA to cells. Our approach is based on the use of a redox-active ferrocene-containing cationic lipid.

The study reported in this paper exploits the physicochemical properties of the redox-active ferrocene-containing lipid bis(11-ferrocenylundecyl)dimethylammonium bromide (BFDMA, Figure 1) [34–36]. This lipid can be reversibly cycled between its reduced state (net charge of +1) and its oxidized state (net charge of +3) by either oxidation or reduction of the ferrocene groups present at the end of each hydrophobic chain [35–41]. Our past studies have demonstrated that the oxidation state of BFDMA significantly affects the interaction of this lipid with DNA [39, 40] and the efficiency with which lipoplexes of BFDMA and DNA transfect cells [37, 38, 41]. In particular, our past studies have identified a range of lipid concentrations over which lipoplexes formed from reduced BFDMA mediate high levels of transgene expression *in vitro*, whereas lipoplexes formed from oxidized BFDMA (over the same range of concentrations) yield negligible levels of transgene expression [37, 38, 41]. Our previous physical characterization experiments also reveal that the oxidation state of BFDMA influences the zeta potentials and nanostructures of lipoplexes formed from BFDMA [39, 40].

The oxidation state of ferrocene-containing surfactants and lipids can be transformed readily and reversibly using electrochemical methods or by using chemical oxidizing and reducing agents [34–46]. In a recent study, we reported the use of glutathione (GSH) to chemically reduce the ferrocenium groups within lipoplexes formed using DNA and oxidized BFDMA (in 1 mM aqueous Li_2SO_4 solution at pH 5.1) [41]. We demonstrated that when these transformed lipoplexes were subsequently introduced to COS-7 cells *in vitro*, they mediated high levels of transgene expression (i.e., levels that were comparable to the levels of transgene expression mediated by lipoplexes formed from reduced BFDMA and DNA). This past study demonstrated that "inactive" lipoplexes of oxidized BFDMA and DNA can be activated by treatment with a chemical reducing agent. However, while these past studies represent a significant step toward the realization of principles that could be used to exert spatial and temporal control over transfection using ferrocene-containing lipids, a number of important issues remain to be addressed. First, as mentioned above, in our previous studies chemical reduction was performed (i) in a simple electrolyte solution (1 mM aqueous Li_2SO_4, as opposed to cell culture media) and (ii) prior to the introduction of the lipoplexes to cells [41]. Second, we also observed that a large molar excess of GSH was required to achieve rapid transformation of oxidized BFDMA within lipoplexes (transformation occurred over ~90 min in the presence of a 10-fold molar excess of GSH, but within seconds to minutes in the presence of a 50-fold molar excess of GSH).

We also note, in this context, that while GSH served as a useful model reducing agent in our initial studies, this molecule is produced in significant concentrations inside cells and is also present at lower concentrations in extracellular environments [47, 48]. In the study reported in this paper, we demonstrate that the rapid and efficient chemical reduction of oxidized BFDMA within lipoplexes can be achieved at significantly lower concentrations using ascorbic acid (vitamin C) as a chemical reducing agent. Ascorbic acid (AA) is a well-known and biologically important chemical reducing agent, but in contrast to GSH it is not synthesized naturally by humans or primates [49]. Below, we demonstrate using cell-based experiments and physicochemical methods of characterization that AA can be used to chemically transform lipoplexes of oxidized BFDMA (via reduction of ferrocenium groups) to "activate" these lipoplexes both in cell culture media and *in the presence of cells* (i.e., by adding small amounts of AA to lipoplex-containing media in which cells are already growing).

Materials and Methods

Materials

BFDMA was synthesized using methods described previously [35]. Ascorbic acid, heparin, and lithium sulfate monohydrate were purchased from Sigma Aldrich (St. Louis, MO). Dodecyltrimethylammonium bromide (DTAB) was purchased from Acros Organics (Morris Plains, NJ). Plasmid DNA constructs encoding enhanced green fluorescent protein [pEGFP-N1 (4.7 kb), >95% supercoiled] and firefly luciferase [pCMV-Luc, >95% supercoiled] were purchased from Elim Biopharmaceuticals, Inc. (San Francisco, CA). Dulbecco's modified Eagle's medium (DMEM), Opti-MEM cell culture medium, phosphate-buffered saline (PBS), fetal bovine serum (FBS), Lipofectamine 2000, Lysotracker Red, Wheat germ agglutinin (WGA)-Alexa Fluor 488, and Hoechst 34580 were purchased from Invitrogen (Carlsbad, CA). Bicinchoninic acid (BCA) protein assay kits were purchased from Pierce (Rockford, IL). Glo Lysis Buffer and Steady-Glo Luciferase Assay kits were purchased from Promega Corporation (Madison, WI). Cy5 Label-IT nucleic acid labeling kits were purchased from Mirus Bio (Madison, WI). Glass inset dishes used for laser scanning confocal microscopy (LSCM) were purchased from MatTek (Ashland, MA). Deionized water (18 MΩ) was used to prepare all buffers and salt solutions.

General Considerations

Electrochemical oxidation of BFDMA was performed as described previously [37–39, 41]. UV/vis absorbance values of lipoplex solutions were monitored using a Beckman Coulter DU520 UV/vis Spectrophotometer (Fullerton, CA). Zeta potential measurements were performed using a Zetasizer 2000HS instrument (Malvern Instruments, Worcestershire, UK). Fluorescence microscopy images used to evaluate the expression of enhanced green fluorescent protein (EGFP) in cell transfection experiments were recorded using an Olympus IX70 microscope and were analyzed using the MetaVue version 7.1.2.0 software package (Molecular Devices; Toronto, Canada). Luminescence and absorbance measurements used to characterize luciferase expression and total cell protein were performed using a PerkinElmer EnVision multilabel plate reader (Luciferase: Em, 700 nm cutoff. BCA: Abs 560 nm). For LSCM experiments, DNA was labeled using a Label-IT nucleic acid labeling kit according to the manufacturer's protocol (labeling density ~100 labels per plasmid). Labeled DNA was purified by ethanol precipitation, and labeling densities were determined using a UV/vis spectrophotometer, as described by the manufacturer. LSCM was performed using a Nikon A1R confocal microscope. LSCM images were processed using *ImageJ* 1.43u (National Institutes of Health; Washington, DC) and Photoshop CS5 (Adobe Systems; San Jose, CA).

Preparation of Lipid and Lipoplex Solutions

Reduced BFDMA solutions (1 mM) were prepared by dissolving reduced BFDMA in aqueous Li_2SO_4 (1 mM, pH 5.1). Oxidized BFDMA solutions were prepared by electrochemical oxidation of solutions of reduced BFDMA. To prepare lipoplex solutions, a solution of plasmid DNA (24 μg/ml in water) was added slowly to the aqueous Li_2SO_4 solution containing an amount of reduced or oxidized BFDMA sufficient to give the final lipid concentrations (and also lipid/DNA charge ratios, CRs) reported in the text. Lipoplex solutions were incubated at room temperature for 20 min before their use in subsequent experiments.

Characterization of the Chemical Reduction of Lipoplexes of Oxidized BFDMA Upon Treatment with AA

For experiments designed to characterize the reduction of oxidized BFDMA within lipoplexes, lipoplexes were diluted in Opti-MEM cell culture medium to a final lipid concentration of 250 μM, and a 10-fold molar excess of AA solution was added. The time-dependent transformation of lipoplexes of oxidized BFDMA upon treatment with AA was monitored by measuring UV/vis absorption spectra at wavelengths ranging from 400–800 nm, in analogy to methods described previously [41]. To facilitate measurements of absorbance, lipoplexes were prepared using a high concentration of BFDMA (250 μM) at lipid/DNA CRs of 1.4:1 and 4.2:1 (for lipoplexes of reduced or oxidized BFDMA, respectively). To eliminate the clouding of solutions of lipoplexes of reduced and oxidized BFDMA or lipoplexes of oxidized BFDMA that were treated with AA, DTAB was added prior to absorption measurements. We note here that DTAB does not absorb light in the range of wavelengths used in these experiments.

Cell Transfection Experiments and Characterization of Transgene Expression

COS-7, HEK 293T/17, HeLa, and NIH 3T3 cells used in cell transfection experiments were grown in clear or opaque polystyrene 96-well culture plates (for experiments using pEGFP-N1 and pCMV-Luc, respectively) at initial seeding densities of 15×10^3, 50×10^3, 24×10^3, and 6×10^3 cells/well, respectively, in 200 μL of growth medium. For each different cell type, the medium used was as follows: 90% DMEM, 10% fetal bovine serum for COS-7 and HEK 293T/17 cells; 90% MEM, 10% fetal bovine serum for HeLa cells, and 90% DMEM,

10% calf bovine serum for NIH 3T3 cells; 100 units/ml penicillin and 100 μg/ml streptomycin were added to media for all cases. After plating, cells were incubated at 37 °C until the cell populations were ~80% confluent. For cell transfection experiments, serum-containing cell culture medium was aspirated and replaced by 200 μL of serum-free medium (Opti-MEM) followed by the addition of 50 μL of lipoplex solutions. After 4 hours of incubation at 37 °C, lipoplex-containing medium was aspirated and replaced with 200 μL of fresh serum-containing medium. Cells were incubated for an additional 48 h and then analyzed for gene expression. For experiments where pEGFP-N1 was used, relative levels of EGFP expression in cells were characterized using fluorescence microscopy. For experiments where pCMV-Luc was used, luciferase protein expression measurements were conducted using luminescence-based luciferase assay kits, according to the manufacturer's specified protocol. Luciferase expression data were normalized against total cell protein in each respective well using a commercially available BCA protein assay kit. All cell transfection experiments were conducted in replicates of six.

Characterization of Internalization of Lipoplexes Using LSCM

COS-7 cells were grown in glass inset confocal microscopy dishes at an initial seeding density of 2.5×10^5 cells/dish in 2 mL of growth medium. Cells were allowed to grow overnight to approximately 80% confluence. Growth medium was then replaced with 2.0 mL of serum-free cell culture medium (Opti-MEM), and 500 μL of lipoplex solutions formulated from BFDMA and pEGFP-N1 (mixture of unlabeled pEGFP-N1 and 20% (w/w) of a pEGFP-N1 labeled with Cy-5) were added. Cells were incubated with lipoplex solutions at 37 °C for 4 hours. Lipoplex solutions were aspirated and then cells were rinsed with 50 U/ml of a heparin solution (in PBS) to promote the removal of extracellular membrane-associated lipoplexes. Cells were then stained with solutions of Hoechst 34580 (nuclear stain), Lysotracker Red (endosome/lysosome stain), and WGA-Alexa Fluor 488 (membrane stain). Internalization of Cy5-labeled DNA was then characterized using LSCM. LSCM images were acquired using a 60x/1.40 NA oil immersion objective. Hoechst 34580, WGA-Alexa Fluor 488, Lysotracker Red, and Cy5-labeled DNA were excited using laser lines at 408, 488, 561 and 638 nm, respectively. Fluorescence emission signals were collected for four individual channels and merged to create four-color images.

Characterization of the Zeta Potentials of Lipoplexes

The zeta potentials of lipoplexes were characterized using a Zetasizer 3000HS (Malvern Instruments, Worcestershire, UK). The analysis of 3 mL samples of lipoplex solutions was performed at ambient temperatures using an electrical potential of 150 V. Five measurements were performed for each lipoplex solution. The Henry equation was used to calculate the zeta potentials from measurements of electrophoretic mobility. In these calculations, the viscosity of the lipoplex solutions was assumed to be same as that of water.

Preparation of Samples of Lipoplexes for Characterization by SANS and Cryo-TEM

Stock solutions of BFDMA (1 mM) were prepared in 1 mM Li_2SO_4. Lipoplex solutions were prepared by adding pEGFP-N1 to stock solutions of BFDMA and then diluting in Opti-MEM cell culture medium. Lipoplexes formed from reduced BFDMA and DNA were prepared at a charge ratio of 1.1:1, and contained the same molar concentrations of BFDMA as complexes formed by oxidized BFDMA and DNA at a charge ratio of 3.3:1. Although these charge ratios were chosen to be close to those used in cell transfection experiments, the absolute concentrations of BFDMA used in the SANS and cryo-TEM measurements (620 to 660 μM) were substantially higher than those used in the transfection experiments. These higher concentrations were necessary to obtain sufficient intensities of scattered neutrons in SANS experiments. To be consistent with the concentrations used in these

SANS measurements and also allow for better sampling, cryo-TEM analyses of BFDMA lipoplexes were also performed at these high lipoplex concentrations.

Characterization of Lipoplexes by Small-Angle Neutron Scattering

SANS measurements were performed using the CG-3 Bio-SANS instrument at the Oak Ridge National Laboratory (ORNL), Oak Ridge, TN. The incident neutron wavelength was on average 6 Å, with a spread in wavelength, $\Delta\lambda/\lambda$, of 15%. Data were recorded at two different sample-to-detector distances (1 and 14.5 m), giving q ranges from 0.490–0.018 and 0.064–0.003 $Å^{-1}$, respectively. To ensure statistically relevant data, at least 10^6 counts were collected for each sample at each detector distance. The samples were contained in quartz cells with a 2 mm path length and placed in a sample chamber held at 25.0 ± 0.1 °C. The data were corrected for detector efficiency, background radiation, empty cell scattering, and incoherent scattering to determine the intensity on an absolute scale [40]. The background scattering from the solvent was subtracted. The processing of data was performed using Igor Pro (WaveMetrics, Lake Oswego, OR) with a program provided by ORNL. Guinier analysis described in detail elsewhere [40, 50] was used to interpret the scattering. Errors reported for d-spacings were calculated directly from q values by assuming a 2% experiment-to-experiment change in Bragg peak position versus q position (via calibration using silver behenate standards).

Characterization of Lipoplexes by Cryo-TEM

Specimens of lipoplexes used for characterization by cryo-TEM were prepared in a controlled environment vitrification (CEVS) system at 25 °C and 100% relative humidity, as previously described [51, 52]. Samples were examined using a Philips CM120 or in a FEI T12 G2 transmission electron microscope, operated at 120 kV, with Oxford CT-3500 or Gatan 626 cooling holders and transfer stations. Specimens were equilibrated in the microscope below −178 °C, and then examined in the low-dose imaging mode to minimize electron beam radiation damage. Images were recorded at a nominal underfocus of 1–2 μm to enhance phase contrast. Images were acquired digitally by a Gatan MultiScan 791 (CM120) or a Gatan US1000 high-resolution (T12) cooled-CCD camera using the DigitalMicrograph software package.

Results and Discussion

Transformation of the Lipoplexes of Oxidized BFDMA by Treatment with Ascorbic Acid

We first conducted experiments to evaluate the extent and rate of reduction of lipoplexes of oxidized BFDMA upon treatment with AA in cell culture medium. For these studies, we selected the serum-free cell culture medium Opti-MEM (pH 7.4), because (i) this culture medium is widely used in *in vitro* cationic lipid-based cell transfection assays, and (ii) our previous cell transfection and physical characterization experiments were also performed using this medium [37–39, 41]. For the experiments presented in this section, we used lipoplexes of reduced or oxidized BFDMA prepared at BFDMA/DNA charge ratios (CRs) of 1.4:1 and 4.2:1, respectively. (We note here that lipoplexes of reduced and oxidized BFDMA prepared at these CRs contain the same molar ratio of BFDMA and DNA, owing to differences in the net charges of reduced (+1) and oxidized (+3) BFDMA.) These CRs were chosen on the basis of our past studies revealing that lipoplexes of reduced BFDMA at a CR of 1.4:1 yield high levels of cell transfection, but that lipoplexes of oxidized BFDMA at a CR of 4.2:1 mediate significantly lower levels of transfection [38, 41].

Figure 2A shows UV/vis absorption spectra of solutions of lipoplexes of reduced BFDMA (black solid line), lipoplexes of oxidized BFDMA (black dashed line), and lipoplexes of oxidized BFDMA treated with a 10-fold molar excess of AA (gray dashed line) in Opti-

MEM cell culture medium. Inspection of these data reveals that upon treatment of lipoplexes of oxidized BFDMA with AA, the absorbance peak at 630 nm, characteristic of oxidized BFDMA, disappeared, and a new maximum in absorbance at 430 nm (characteristic of the max. absorbance of reduced BFDMA) appeared. The overall shape of the absorption spectrum of lipoplexes of oxidized BFDMA treated with AA was similar to that of lipoplexes of reduced BFDMA. Additional characterization of the time dependent disappearance of the peak in absorbance at 630 nm demonstrated that the AA-mediated reduction of lipoplexes occurred over a period of ~1 min (Figure 2B). These observations demonstrate that AA can be used to reduce the ferrocenium groups of oxidized BFDMA in lipoplexes at rates that are significantly higher than those that are possible using GSH (e.g., reduction occurred over ~90 min in the presence of 10-fold molar excess of GSH [41]).

Treatment of Lipoplexes of Oxidized BFDMA with AA in the Presence of Cells Activates Lipoplexes Toward Transfection

In our previous study, we demonstrated that GSH could be used to chemically transform inactive lipoplexes of oxidized BFDMA to lipoplex solutions capable of mediating levels of transgene expression comparable to those promoted by lipoplexes of reduced BFDMA (at several lipid/DNA CRs) [41]. In that study, chemical transformations of oxidized BFDMA lipoplexes were performed in 1 mM aqueous Li_2SO_4 prior to the introduction of the lipoplexes to cells [41]. In this current study, we sought to determine whether it was possible to perform the chemical transformation and, thus, the activation of inactive lipoplexes of oxidized BFDMA in cell culture media (Opti-MEM) and directly in the presence of cells. Here, we note that Opti-MEM differs from the Li_2SO_4 solutions used in our past studies in two important ways. First, the Li_2SO_4 solutions used in our past studies were prepared at pH 5.1 (this pH was chosen based on conditions required for the bulk electrolysis of BFDMA), but Opti-MEM is at physiological pH (pH 7.4). Second, Opti-MEM is a far more complex medium (e.g., it contains salts, trace elements, growth factors, and proteins) than aqueous Li_2SO_4 solution.

On the basis of these differences, we first sought to determine whether the addition of AA to lipoplexes of oxidized BFDMA in Opti-MEM cell culture medium and the presence of cells would lead to the activation of lipoplexes and result in high levels of cell transfection. To this end, we performed a series of qualitative gene expression assays using the COS-7 cell line and lipoplexes prepared from BFDMA and a plasmid DNA construct (pEGFP-N1) encoding enhanced green fluorescent protein (EGFP). For these experiments, we used lipoplexes prepared at BFDMA/DNA CRs that were identical to those used in the experiments described above (i.e., BFDMA/DNA CRs of 1.4:1 and 4.2:1 for lipoplexes of reduced and oxidized BFDMA, respectively), but at lower overall BFDMA concentrations (10 μM). (See Materials and Methods for additional details regarding these cell transfection experiments). Immediately following the introduction of lipoplexes of oxidized BFDMA to cells incubated in Opti-MEM, AA was added to the media and stirred gently using a pipette.

Figure 3 shows representative fluorescence micrographs of COS-7 cells 48 h after incubation with either lipoplexes of (A) reduced BFDMA, (B) oxidized BFDMA, or (C) lipoplexes of oxidized BFDMA treated with AA. Inspection of these images reveals that lipoplexes of reduced BFDMA mediated high levels of EGFP expression, while lipoplexes of oxidized BFDMA yielded significantly lower levels of expression. These results are consistent with those of our past studies [37, 38, 41]. Further inspection of Figure 3C, however, reveals that the lipoplexes of oxidized BFDMA that were treated with AA after addition to cells mediated levels of transgene expression that were qualitatively similar to those mediated by lipoplexes of reduced BFDMA. When combined, these results suggest that the addition of AA to the extracellular environment can be used to transform otherwise

inactive lipoplexes of oxidized BFDMA into active lipoplexes that mediate high levels of transfection.

To confirm the results above and characterize relative levels of transgene expression quantitatively, we performed a second series of transfection experiments using lipoplexes formulated using BFDMA and a plasmid encoding firefly luciferase (pCMV-Luc) over a range of lipid concentrations (e.g., from 8 to 40 μM). These lipid concentrations correspond to lipid/DNA CRs ranging from 1.1:1 to 5.5:1 (for lipoplexes of reduced BFDMA) and 3.3:1 to 16.5:1 (for lipoplexes of oxidized BFDMA). These BFDMA concentrations (and thus BFDMA/DNA CRs) were chosen to permit comparisons to broader ranges of lipid concentrations used in our previous studies [37, 38, 41].

Figure 4A shows levels of luciferase expression (expressed as relative light units normalized to total concentration of cell protein) mediated by lipoplexes of BFDMA in the COS-7 cell line. The results of this experiment (Figure 4A) reveal that lipoplexes of reduced BFDMA (black bars) mediate significantly higher levels of transgene expression than lipoplexes of oxidized BFDMA (gray bars) at all of the BFDMA concentrations investigated. These results are generally similar to the results of our past studies [37, 38, 41]. Inspection of the luciferase expression data corresponding to lipoplexes of oxidized BFDMA treated with AA (white bars), however, reveals that these lipoplexes are able to mediate levels of transgene expression that are significantly higher than those mediated by lipoplexes of oxidized BFDMA (gray bars), particularly at BFDMA concentrations of 10 and 20 μM. The relative decrease in the level of expression of luciferase that is measured when using 40 μM BFDMA is due to the cytotoxicity of BFDMA at this higher concentration, as detailed in our past studies [38, 41]. We also note here that control experiments using (i) solutions of AA alone or (ii) mixtures of AA and DNA in the absence of BFDMA did not result in levels of transgene expression comparable to those mediated by lipoplexes of oxidized BFDMA treated with AA (data not shown). Furthermore, the addition of a 10-fold molar excess of AA to lipoplexes of reduced BFDMA did not affect the level of transgene expression mediated by these lipoplexes.

These results, when combined, suggest that the increased levels of cell transfection that are observed to accompany the addition of AA to lipoplexes of oxidized BFDMA are due to the reduction of oxidized BFDMA within lipoplexes (and that this is not the result of other potential influences of AA on cell behavior). In conclusion, the results shown in Figures 3 and 4A demonstrate that AA is able to transform (or activate) lipoplexes of oxidized BFDMA in the presence of cells, and that this transformation leads to lipoplexes that promote high levels of transgene expression in the COS-7 cell line. Finally, we note that levels of transgene expression mediated by lipoplexes of oxidized BFDMA treated with AA are lower than those mediated by lipoplexes of reduced BFDMA. Physicochemical factors and differences in lipoplex structure that could underlie these differences in levels of cell transfection are discussed in additional detail below.

We selected COS-7 cells for use in the initial studies above for two important reasons. First, the use of COS-7 cells allowed us to compare the results of this current study to those of our past investigations using this cell line [37, 38, 41]. Second, this cell line is generally considered to be easy to transfect, and, as such, provides a more challenging test of lipoplex “inactivity” (that is, our results demonstrate that lipoplexes of oxidized BFDMA (i.e., in an “off” state) transfect very poorly using a cell line that is otherwise regarded to be relatively easy to transfect [53]). We performed additional experiments similar to those described above to investigate the ability of lipoplexes of BFDMA to transfect three additional cell lines (HEK 293T/17, HeLa, and NIH 3T3 cells) used widely for the characterization of non-viral gene delivery systems. Quantitative luciferase-based transfection experiments were

conducted in these additional cell lines using concentrations of BFDMA, lipid/DNA CRs, and other conditions identical to those used for transfection assays using COS-7 cells above.

Figures 4B–D show plots of normalized luciferase expression in (B) HEK 293T/17, (C) HeLa and (D) NIH 3T3 cells after treatment with lipoplexes of reduced BFDMA (black bars), oxidized BFDMA (gray bars), or lipoplexes of oxidized BFDMA treated with AA (white bars). Inspection of these data reveals that lipoplexes of reduced BFDMA (black bars) were able to mediate significant levels of transfection in these cell lines at lipid concentrations ranging from 8 μM to 20 μM (albeit at absolute levels of expression that were different for each cell type; we return to these observations again below). In contrast, lipoplexes of oxidized BFDMA (gray bars) mediated levels of transfection that were significantly lower than those mediated by lipoplexes of reduced BFDMA. These results are generally consistent with the results of our current (Figure 4A) and past studies using COS-7 cells [37, 38, 41], and lead to two important conclusions: (i) that the ability of reduced BFDMA to transfect cells is not limited to transfection of the COS-7 cell line, and (ii) that the large differences in transfection observed between lipoplexes of reduced and oxidized BDFMA are maintained across a more diverse panel of cell types. Finally, these results also reveal that the addition of AA can be used to transform lipoplexes of oxidized BFDMA (gray bars) to lipoplexes (white bars) that are able to mediate significantly higher levels of cell transfection at BFDMA concentrations of 10 and 20 μM.

As described above, the absolute levels of luciferase expression mediated by lipoplexes of reduced BFDMA and lipoplexes of oxidized BFDMA treated with AA varied considerably for each cell type. The data presented in Figure 4, for example, demonstrate that levels of luciferase expression observed in the COS-7 and HEK 293T/17 cell lines were much higher (on the order of 10^7 – 10^9 RLU/mg protein, depending on BFDMA concentration) compared to levels of expression in HeLa and NIH 3T3 cells (e.g., on the order of 10^5 RLU/mg protein under otherwise identical conditions). These results are consistent with the results of other past studies demonstrating that levels of gene expression in HeLa and NIH 3T3 cells are lower than those in COS-7 and HEK 293T/17 cells [25, 28, 54]. Although many different factors could contribute to these large variations in transgene expression, the higher levels of expression observed in the COS-7 and HEK 293T/17 cells here also likely arise, at least in part, from the fact that these two transformed cell lines express the SV40 large T antigen [55, 56]. Expression of this antigen is known to result in increased expression of gene products of plasmids that contain the SV40 origin of replication (as contained in the two plasmid constructs used in this study) [55]. We note also that these current experiments were designed to investigate and screen the ability of BFDMA to transfect cells over a broad range of lipid concentrations. It is likely, however, that additional optimization studies could lead to formulations and experimental conditions that lead to higher absolute levels of transfection in these four cell types. In the context of this current study, however, we note that the primary significance of the results reported here lies not in comparisons of absolute levels of transgene expression, but in the observations that both (i) the fundamental influence of the redox state of BFDMA on cell transfection and (ii) the ability to chemically transform this redox state in a useful way by treatment with AA are preserved across a broader range of different cell types.

Characterization of Cellular Internalization and Zeta Potentials of Lipoplexes of Oxidized BFDMA Treated with AA

We used laser scanning confocal microscopy (LSCM) and lipoplexes prepared using plasmid DNA labeled with a Cy-5 fluorescent label to characterize differences in the extents to which the lipoplexes reported above were internalized by COS-7 cells. Guided by the results of our transfection experiments, the concentration of BFDMA used in these experiments was 10 μM. The cells were incubated with lipoplexes of (i) reduced BFDMA,

(ii) oxidized BFDMA, or (iii) lipoplexes of oxidized BFDMA treated with AA immediately after addition to cells. After a 4 h incubation period, cells were rinsed extensively with a solution of heparin (50 U/ml) to promote the removal of lipoplexes associated with (i.e., bound to) cell membranes. Figure 5 shows LSCM images of the cells in these experiments. In these images blue, green, red and gray signals correspond to Lysotracker Red (endosome/lysosome stain), WGA-Alexa Fluor 488 (membrane stain), Cy5-labeled DNA, and Hoechst 34580 (nuclear stain), respectively. Membrane-associated red structures correspond to lipoplexes associated with cell membranes that were not removed by rinsing steps mentioned above.

The image in Figure 5A shows cells incubated with lipoplexes of reduced BFDMA for 4 hours. Inspection of this image reveals significant internalization of lipoplexes, and that DNA is present (i) as large aggregates which appear to be associated with the cell membrane (e.g., thick white arrows), (ii) inside the cells either in endosomes and/or lysosomes (e.g., thin white arrows; when blue signal corresponding to endosomes and/or lysosomes is merged with the red signal corresponding to Cy-5 labeled DNA, magenta spots are formed), and (iii) inside cells but not in acidic endosomes and/or lysosomes (e.g., white arrowheads). In contrast, inspection of the representative image in Figure 5B, corresponding to cells treated with lipoplexes of oxidized BFDMA for 4 h, shows very low levels of internalized DNA (e.g., white arrowhead). The image in Figure 5C, which corresponds to cells incubated with lipoplexes of oxidized BFDMA that were subsequently treated with AA, reveals high levels of internalized DNA and that the internalized DNA is located either in endosomes and/or lysosomes (e.g., thin white arrows) or in the cytosol (e.g., white arrowheads). A comparison of these results to the image shown in Figure 5A also reveals that fewer large aggregates are associated with the cell membrane (although several smaller membrane-associated aggregates are observed; Figure 5C, e.g., white arrows). The results shown in Figures 5A and B are in general agreement with the results of our past studies [41] and demonstrate that redox state of BFDMA significantly influences levels of cell transfection by changing the extents to which lipoplexes are internalized (or not internalized) by cells. The observation that lipoplexes of oxidized BFDMA treated with AA are internalized readily by cells correlates with the observation of higher levels of transfection (e.g., Figures 3 and 4) and provides additional support for the view that lipoplexes of oxidized BFDMA can be activated toward transfection by the chemical reduction or transformation of the lipoplexes in the *extracellular* environment (and prior to internalization by cells).

Past studies have demonstrated that the efficiency with which lipoplexes are internalized by cells tends to increase with increases in the zeta potentials of the lipoplexes [57, 58]. To provide insight into changes in the physical properties of BFDMA lipoplexes that could underlie the changes in internalization and transgene expression described above, we performed a series of experiments to characterize the zeta potentials of BFDMA lipoplexes in Opti-MEM cell culture medium. These experiments were conducted using lipoplexes formed at lipid concentrations and BFDMA/DNA CRs identical to those used in the transfection and internalization experiments described above (i.e., at a BFDMA concentration of 10 μM and at a BFDMA/DNA CR of 1.4:1 and 4.2:1 for lipoplexes of reduced and oxidized BFDMA, respectively).

Table 1 shows the results of zeta potential measurements of either lipoplexes of reduced BFDMA, oxidized BFDMA, or lipoplexes of oxidized BFDMA treated with AA in Opti-MEM cell culture medium. These data reveal that the average zeta potential of lipoplexes of reduced BFDMA (which mediated high levels of internalization and transfection in the above experiments) was approximately −17 mV under these conditions. In contrast, the average zeta potential of lipoplexes of oxidized BFDMA (which were not internalized readily and did not mediate high levels of cell transfection) was considerably more negative

(approximately −34 mV). The average zeta potential of lipoplexes of oxidized BFDMA that were treated with AA (approximately −21 mV), however, was less negative than that of lipoplexes of oxidized BFDMA and, in general, closer in magnitude to that of lipoplexes of reduced BFDMA. We note that while the zeta potentials of lipoplexes of reduced BFDMA and lipoplexes of oxidized BFDMA treated with AA were not measured to be positive under these conditions (e.g., in Opti-MEM), these two types of lipoplexes did result in high levels of transfection and internalization in the experiments above. It is possible that the less-negative zeta potentials of these lipoplexes contribute to more efficient internalization and transfection by facilitating more favorable electrostatic interactions with negatively charged cell membranes, although we note that these current results do not rule out other factors that could lead to differences in internalization. In the section below, we describe the results of other physicochemical and nanostructural characteristics that could also contribute to observed differences in internalization and/or transfection.

Characterization of Lipoplexes using SANS and Cryo-TEM

We used SANS and cryo-TEM to provide additional insight into changes in the nanostructures of lipoplexes of oxidized BFDMA that could occur upon the addition of AA. These characterization experiments were performed in Opti-MEM cell culture medium using lipoplexes formulated at BFDMA/DNA CRs used in the transfection analyses described above (i.e., at a BFDMA/DNA CR of 1.1:1 and 3.3:1 for lipoplexes of reduced BFDMA and oxidized BFDMA, respectively). However, as described above in the Materials and Methods section, these experiments were performed at higher overall lipoplex concentrations to obtain sufficient intensities of scattered neutrons in SANS experiments. We note that these CRs do not correspond to those that lead to the highest levels of cell transfection in Figure 4; these CRs were chosen to permit comparison to the SANS and cryo-TEM results reported in our past study on the characterization of lipoplexes of BFDMA and DNA at these CRs in 1 mM Li_2SO_4 [40]. The results of this past study demonstrated that the nanostructures of lipoplexes of BFDMA did not change substantially as CRs were varied (at least for lipoplexes of reduced BFDMA).

Figure 6 shows SANS spectra of lipoplexes of reduced BFDMA (solid black triangles), lipoplexes of oxidized BFDMA (solid gray triangles), and lipoplexes of oxidized BFDMA that were treated with AA (open black triangles). The inset in Figure 6 shows the Bragg peaks observed at q=0.12 $Å^{-1}$ for these solutions. In both plots, the SANS spectra corresponding to solutions of lipoplexes of oxidized BFDMA and lipoplexes of oxidized BFDMA treated with AA were offset by a scale factor of 1.2 to facilitate comparison to the spectrum of lipoplexes of reduced BFDMA. The SANS spectrum of the lipoplexes of reduced BFDMA (solid black triangles) exhibits a single peak at q=0.12 $Å^{-1}$ (see Figure 6 inset), which corresponds to a nanostructure with a periodicity of 5.2 nm. This periodicity is the same as that determined previously by us to correspond to multi-lamellar complexes of BFDMA and DNA [40], and is consistent with a model (informed by cryo-TEM images; see Figure 7A, below) in which double-stranded DNA and D_2O (combined thickness of 2.5 nm) are intercalated between lipid bilayers (lipid thickness is estimated to be 2.7 nm). The presence of a single Bragg peak suggests that this periodic nanostructure does not extend over large distances. We also note here that these results obtained in Opti-MEM cell culture medium are similar to SANS results reported previously by our group using lipoplexes of BFDMA prepared in 1 mM Li_2SO_4 (i.e., in the absence of Opti-MEM) [40]. This result indicates that the periodicity of the nanostructure formed by reduced BFDMA and DNA in simple electrolytes is not disrupted by the higher ionic strength and more complex composition of Opti-MEM cell culture medium. Further inspection of the SANS data for these lipoplexes (solid black triangles) in the low q region of the spectrum reveals a q^{-4} dependence that is consistent with the presence of polydisperse multilamellar vesicles [40].

Next, we used SANS to characterize the nanostructures of lipoplexes of oxidized BFDMA in OptiMEM cell culture medium (Figure 6, solid gray triangles). For the solutions of lipoplexes of oxidized BFDMA, a Bragg peak with a low intensity was obtained (see Figure 6 inset, solid gray triangles) at the same value of q (0.12 $Å^{-1}$) at which the Bragg peak of the lipoplexes of reduced BFDMA was observed. The low intensity of this Bragg peak suggests that relatively few periodic structures are present in solution and/or that the range of ordering of the periodic structures is short (as compared to lipoplexes of reduced BFDMA). In our previous study, in which we analyzed lipoplexes of oxidized BFDMA in 1 mM Li_2SO_4 (i.e., in the absence of Opti-MEM), no Bragg peak was observed in the SANS spectrum, indicating the absence of detectable periodic nanostructure in the solutions of the lipoplexes of oxidized BFDMA in 1 mM Li_2SO_4 [40]. However, the development of a Bragg peak for the lipoplexes of oxidized BFDMA in Opti-MEM cell culture medium suggests that the high ionic strength and/or the other components of Opti-MEM promote formation of ordered nanostructures (see cryo-TEM images of lipoplexes of oxidized BFDMA (Figure 7B), which demonstrates the formation of nanostructures with short range of ordering at the edges of loose aggregate structures). We also note that the SANS spectrum of lipoplexes of oxidized BFDMA in the low q region follows a q dependence of $q^{-2.8}$, consistent with the presence of loose aggregate structures [40, 59]. These data, when combined, suggest that lipoplexes of oxidized BFDMA in Opti-MEM cell culture medium form both loose aggregates and periodic nanostructures with a short range of ordering.

Figure 6 also shows the SANS spectrum of lipoplexes of oxidized BFDMA that were treated with AA (open black triangles). These data reveal a Bragg peak at the same position as the peak for lipoplexes of reduced or oxidized BFDMA (q=0.12 $Å^{-1}$; see Figure 6 inset). In contrast to the spectrum observed for lipoplexes of oxidized BFDMA, the height of the Bragg peak following treatment with AA was similar to the height of the Bragg peak observed for lipoplexes of reduced BFDMA. This result suggests that the periodicity of the nanostructures of the lipoplexes of reduced BFDMA and lipoplexes of oxidized BFDMA treated with AA are similar. Furthermore, scattering from lipoplexes of oxidized BFDMA treated with AA in the low q-region of the spectrum has a q dependence that is close to $q^{-3.5}$, a dependence that is close to that observed for lipoplexes of reduced BFDMA.

We also performed cryo-TEM experiments to provide complementary insight into differences in the nanostructures of these lipoplexes (Figure 7). Cryo-TEM characterization of lipoplexes of reduced BFDMA (Figure 7A) revealed spherically shaped, onion-like multilamellar structures (white asterisks) and a physical picture of the nanostructures of these lipoplexes that was generally consistent with the results of SANS measurements described above. We also observed partially disassociated structures and DNA threadlike structures, however their presence was rare and the majority of the lipoplexes were intact onion-like multilamellar structures with varying numbers of shells per aggregate. The disassociation could result from additional competitive interactions of lipoplexes with components of Opti-MEM cell culture medium. The structural characteristics of the lipoplexes of reduced BFDMA were consistent with the presence of a Bragg peak and also a q dependence of −4 in the low q region in the SANS spectrum of these complexes (Figure 6, solid black triangles).

Cryo-TEM characterization of lipoplexes of oxidized BFDMA (Figure 7B) revealed the presence of large amorphous aggregates (asterisk) and few isolated lamellar structures, sometimes located at the edges of these aggregates (white arrows). In general, these results are consistent with the q dependence of −2.8 in the low q region and the presence of a low intensity Bragg peak, respectively, in the SANS spectrum of these lipoplexes. Most of these lamellar structures (composed of 2–3 layers of lamellae) did not form onion-like spheres. We note again that these amorphous nanostructures are different from those observed by

cryo-TEM of lipoplexes of oxidized BFDMA in Li_2SO_4 [40] (the cryo-TEM images of lipoplexes of oxidized BFDMA in Li_2SO_4 show predominantly dense amorphous aggregates without any periodic nanostructures). Finally, arrowheads in Figure 7B point to fuzzy edges of the lamellar aggregates, where DNA threadlike structures emerge. This may also indicate dissociation of DNA from these aggregates in Opti-MEM cell culture medium.

Cryo-TEM images of lipoplexes of oxidized BFDMA treated with AA (Figures 7C and 7D) reveal the coexistence of amorphous structures, multilamellar aggregates, and DNA threadlike structures. The multilamellar aggregates are either non-spherical (Figure 7C and 7D; white arrows), or consist of small spherical onion-like structures (Figure 7C, asterisk). The non-spherical multilamellar structures were composed of several layers of lamellae, and were curved (in contrast to the structures observed in oxidized BFDMA lipoplexes). The presence of multilamellar nanostructures (Figure 7C and 7D) is consistent with the presence of a Bragg peak in the SANS spectrum of these lipoplexes. Similar to the samples of lipoplexes of oxidized BFDMA described above, DNA threadlike structures (Figure 7C and 7D, arrowheads) were also observed in areas near the lipoplexes. In both cases, we also observed DNA threads dispersed in the solution in areas that did not contain other aggregates (e.g., see Figure S1 of the Supplementary Data). In contrast, the amorphous structures (Figure 7D, black arrows) observed for lipoplexes of oxidized BFDMA treated with AA differ from those observed in the samples of lipoplexes of oxidized BFDMA; they are less dense, and show better contrast and order.

In conclusion, the results of SANS and cryo-TEM analyses (Figures 6 and 7) demonstrate that lipoplexes of reduced and oxidized BFDMA, or lipoplexes of oxidized BFDMA treated with AA, form nanostructures with different characteristics in Opti-MEM cell culture medium. The lipoplexes of reduced BFDMA form mostly onion-like multilamellar structures. In contrast, lipoplexes of oxidized BFDMA form mostly amorphous aggregates, although some lamellar structures (composed of 2–3 layers of lamellae) at the edges of the amorphous structures were observed. The formation of these lamellar structures could be triggered by the pH or the components of Opti-MEM, since in our previous cryo-TEM analysis of lipoplexes of oxidized BFDMA in 1 mM aqueous Li_2SO_4, we did not observe these ordered structures at the edges of amorphous aggregates. Finally, we observed that the treatment of lipoplexes of oxidized BFDMA with AA in Opti-MEM cell culture medium leads to formation of small onion-like and curved multilamellar structures (i.e., a nanostructure that is similar to lipoplexes of reduced BFDMA).

Conclusions

We have demonstrated that AA can be used as a chemical reducing agent to activate otherwise inactive lipoplexes of oxidized BFDMA in the presence of cells. Our results establish that treatment with AA results in the rapid reduction of the ferrocenium groups of oxidized BFDMA, and that the resulting lipoplexes of reduced BFDMA mediate significant levels of cell transfection in a panel of several different cell lines (COS-7, HEK 293T/17, HeLa, and NIH 3T3 cell lines). Characterization by confocal microscopy and measurements of the zeta potentials of lipoplexes suggested that the large differences in cell transfection mediated by lipoplexes of oxidized BFDMA and lipoplexes of oxidized BFDMA treated with AA resulted from significant differences in the extents to which these lipoplexes were internalized by cells. Our results also demonstrate that these differences in transfection are a result of changes in the oxidation state of BFDMA that occur in the extracellular environment (that is, prior to the internalization of lipoplexes by cells). Additional characterization by SANS and cryo-TEM measurements revealed changes in the nanostructures of lipoplexes of oxidized BFDMA upon treatment with AA from aggregates that were generally amorphous to aggregates with a more extensive multilamellar

nanostructure. When combined, the results of this study provide guidance for the design of redox-active lipids for cell transfection, and provide the basis of an approach for the extracellular activation of lipoplexes that could lead to new methods for exerting spatial and/or temporal control over the transfection of cells *in vitro*.

Supplementary Material

Refer to Web version on PubMed Central for supplementary material.

Acknowledgments

Financial support was provided by the NIH (1 R21 EB006168) and the National Science Foundation (CBET-0754921). We thank Lance Rodenkirch, and the W. M. Keck Center for Biological Imaging at the UW-Madison for access to and assistance with confocal microscopy facilities. We gratefully acknowledge the support of the Oak Ridge National Laboratory in providing the neutron facilities. The cryo-TEM work was carried out at the Technion Soft Matter Electron Microscopy Laboratory with the financial support of the Technion Russell Berrie Nanotechnology Institute (RBNI).

References

1. Felgner PL, Gadek TR, Holm M, Roman R, Chan HW, Wenz M, Northrop JP, Ringold GM, Danielsen M. Lipofection - a highly efficient, lipid-mediated DNA-transfection procedure. Proc Natl Acad Sci U S A. 1987; 84:7413–7417. [PubMed: 2823261]
2. Zabner J. Cationic lipids used in gene transfer. Adv Drug Deliv Rev. 1997; 27:17–28. [PubMed: 10837548]
3. Kabanov, AV.; Felgner, PL.; Seymour, LW. Self-assembling complexes for gene delivery: From laboratory to clinical trial. John Wiley and Sons; New York: 1998.
4. de Lima MCP, Neves S, Filipe A, Duzgunes N, Simoes S. Cationic liposomes for gene delivery: From biophysics to biological applications. Curr Med Chem. 2003; 10:1221–1231. [PubMed: 12678796]
5. Wasungu L, Hoekstra D. Cationic lipids, lipoplexes and intracellular delivery of genes. J Control Release. 2006; 116:255–264. [PubMed: 16914222]
6. de Ilarduya CT, Sun Y, Duzgunes N. Gene delivery by lipoplexes and polyplexes. Eur J Pharm Sci. 2010; 40:159–170. [PubMed: 20359532]
7. Lasic DD, Templeton NS. Liposomes in gene therapy. Adv Drug Deliv Rev. 1996; 20:221–266.
8. Zhang SB, Xu YM, Wang B, Qiao WH, Liu DL, Li ZS. Cationic compounds used in lipoplexes and polyplexes for gene delivery. J Control Release. 2004; 100:165–180. [PubMed: 15544865]
9. Lewis JG, Lin KY, Kothavale A, Flanagan WM, Matteucci MD, DePrince RB, Mook RA, Hendren RW, Wagner RW. A serum-resistant cytofectin for cellular delivery of antisense oligodeoxynucleotides and plasmid DNA. Proc Natl Acad Sci U S A. 1996; 93:3176–3181. [PubMed: 8622909]
10. Wheeler JJ, Palmer L, Ossanlou M, MacLachlan I, Graham RW, Zhang YP, Hope MJ, Scherrer P, Cullis PR. Stabilized plasmid-lipid particles: Construction and characterization. Gene Ther. 1999; 6:271–281. [PubMed: 10435112]
11. Mustapa MFM, Grosse SM, Kudsiova L, Elbs M, Raiber EA, Wong JB, Brain APR, Armer HEJ, Warley A, Keppler M, Ng T, Lawrence MJ, Hart SL, Hailes HC, Tabor AB. Stabilized integrin-targeting ternary lpd (lipopolyplex) vectors for gene delivery designed to disassemble within the target cell. Bioconjug Chem. 2009; 20:518–532. [PubMed: 19228071]
12. Wetzer B, Byk G, Frederic M, Airiau M, Blanche F, Pitard B, Scherman D. Reducible cationic lipids for gene transfer. Biochem J. 2001; 356:747–756. [PubMed: 11389682]
13. Tang FX, Hughes JA. Introduction of a disulfide bond into a cationic lipid enhances transgene expression of plasmid DNA. Biochem Biophys Res Commun. 1998; 242:141–145. [PubMed: 9439625]

14. Tang FX, Hughes JA. Use of dithiodiglycolic acid as a tether for cationic lipids decreases the cytotoxicity and increases transgene expression of plasmid DNA in vitro. Bioconjug Chem. 1999; 10:791–796. [PubMed: 10502344]
15. Guo X, Szoka FC. Chemical approaches to triggerable lipid vesicles for drug and gene delivery. Acc Chem Res. 2003; 36:335–341. [PubMed: 12755643]
16. Huang ZH, Li WJ, MacKay JA, Szoka FC. Thiocholesterol-based lipids for ordered assembly of bioresponsive gene carriers. Mol Ther. 2005; 11:409–417. [PubMed: 15727937]
17. Budker V, Gurevich V, Hagstrom JE, Bortzov F, Wolff JA. Ph-sensitive, cationic liposomes: A new synthetic virus-like vector. Nat Biotechnol. 1996; 14:760–764. [PubMed: 9630986]
18. Gerasimov OV, Boomer JA, Qualls MM, Thompson DH. Cytosolic drug delivery using ph- and light-sensitive liposomes. Adv Drug Deliv Rev. 1999; 38:317–338. [PubMed: 10837763]
19. Zhu J, Munn RJ, Nantz MH. Self-cleaving ortho ester lipids: A new class of ph-vulnerable amphiphiles. J Am Chem Soc. 2000; 122:2645–2646.
20. Meers P. Enzyme-activated targeting of liposomes. Adv Drug Deliv Rev. 2001; 53:265–272. [PubMed: 11744171]
21. Prata CAH, Zhao YX, Barthelemy P, Li YG, Luo D, McIntosh TJ, Lee SJ, Grinstaff MW. Charge-reversal amphiphlies for gene delivery. J Am Chem Soc. 2004; 126:12196–12197. [PubMed: 15453715]
22. Nagasaki T, Taniguchi A, Tamagaki S. Photoenhancement of transfection efficiency using novel cationic lipids having a photocleavable spacer. Bioconjug Chem. 2003; 14:513–516. [PubMed: 12757373]
23. Wolff JA, Rozema DB. Breaking the bonds: Non-viral vectors become chemically dynamic. Mol Ther. 2008; 16:8–15. [PubMed: 17955026]
24. Liu YC, Le Ny ALM, Schmidt J, Talmon Y, Chmelka BF, Lee CT. Photo-assisted gene delivery using light-responsive catanionic vesicles. Langmuir. 2009; 25:5713–5724. [PubMed: 19435291]
25. Ziauddin J, Sabatini DM. Microarrays of cells expressing defined cDNAs. Nature. 2001; 411:107–110. [PubMed: 11333987]
26. Yamauchi F, Kato K, Iwata H. Micropatterned, self-assembled monolayers for fabrication of transfected cell microarrays. Biochim Biophys Acta Gen Subj. 2004; 1672:138–147.
27. Chang FH, Lee CH, Chen MT, Kuo CC, Chiang YL, Hang CY, Roffler S. Surfection: A new platform for transfected cell arrays. Nucleic Acids Res. 2004; 32:e33. [PubMed: 14973329]
28. Isalan M, Santori MI, Gonzalez C, Serrano L. Localized transfection on arrays of magnetic beads coated with PCR products. Nat Methods. 2005; 2:113–118. [PubMed: 15782208]
29. Hook AL, Thissen H, Voelcker NH. Advanced substrate fabrication for cell microarrays. Biomacromolecules. 2009; 10:573–579. [PubMed: 19159278]
30. Saltzman WM. Delivering tissue regeneration. Nat Biotechnol. 1999; 17:534–535. [PubMed: 10385312]
31. Shea LD, Smiley E, Bonadio J, Mooney DJ. DNA delivery from polymer matrices for tissue engineering. Nat Biotechnol. 1999; 17:551–554. [PubMed: 10385318]
32. Shepard JA, Huang A, Shikanov A, Shea LD. Balancing cell migration with matrix degradation enhances gene delivery to cells cultured three-dimensionally within hydrogels. J Control Release. 2010; 146:128–135. [PubMed: 20450944]
33. Yang F, Cho SW, Son SM, Bogatyrev SR, Singh D, Green JJ, Mei Y, Park S, Bhang SH, Kim BS, Langer R, Anderson DG. Genetic engineering of human stem cells for enhanced angiogenesis using biodegradable polymeric nanoparticles. Proc Natl Acad Sci U S A. 2010; 107:3317–3322. [PubMed: 19805054]
34. Kakizawa Y, Sakai H, Nishiyama K, Abe M, Shoji H, Kondo Y, Yoshino N. Solution properties of double-tailed cationic surfactants having ferrocenyl groups in their hydrophobic moieties. Langmuir. 1996; 12:921–924.
35. Yoshino N, Shoji H, Kondo Y, Kakizawa Y, Sakai H, Abe M. Syntheses of cationic surfactants having two ferrocenylalkyl chains. J Jpn Oil Chem Soc. 1996; 45:769–775.

36. Kakizawa Y, Sakai H, Yamaguchi A, Kondo Y, Yoshino N, Abe M. Electrochemical control of vesicle formation with a double-tailed cationic surfactant bearing ferrocenyl moieties. Langmuir. 2001; 17:8044–8048.
37. Abbott NL, Jewell CM, Hays ME, Kondo Y, Lynn DM. Ferrocene-containing cationic lipids: Influence of redox state on cell transfection. J Am Chem Soc. 2005; 127:11576–11577. [PubMed: 16104714]
38. Jewell CM, Hays ME, Kondo Y, Abbott NL, Lynn DM. Ferrocene-containing cationic lipids for the delivery of DNA: Oxidation state determines transfection activity. J Control Release. 2006; 112:129–138. [PubMed: 16529838]
39. Hays ME, Jewell CM, Kondo Y, Lynn DM, Abbott NL. Lipoplexes formed by DNA and ferrocenyl lipids: Effect of lipid oxidation state on size, internal dynamics, and zeta-potential. Biophys J. 2007; 93:4414–4424. [PubMed: 17720731]
40. Pizzey CL, Jewell CM, Hays ME, Lynn DM, Abbott NL, Kondo Y, Golan S, Tahnon Y. Characterization of the nanostructure of complexes formed by a redox-active cationic lipid and DNA. J Phys Chem B. 2008; 112:5849–5857. [PubMed: 18419168]
41. Jewell CM, Hays ME, Kondo Y, Abbott NL, Lynn DM. Chemical activation of lipoplexes formed from DNA and a redox-active, ferrocene-containing cationic lipid. Bioconjug Chem. 2008; 19:2120–2128. [PubMed: 18831573]
42. Saji T, Hoshino K, Aoyagui S. Reversible formation and disruption of micelles by control of the redox state of the head group. J Am Chem Soc. 1985; 107:6865–6868.
43. Gallardo BS, Hwa MJ, Abbott NL. In-situ and reversible control of the surface-activity of ferrocenyl surfactants in aqueous-solutions. Langmuir. 1995; 11:4209–4212.
44. Bennett DE, Gallardo BS, Abbott NL. Dispensing surfactants from electrodes: Marangoni phenomenon at the surface of aqueous solutions of (11-ferrocenylundecyl)trimethylammonium bromide. J Am Chem Soc. 1996; 118:6499–6505.
45. Gallardo BS, Gupta VK, Eagerton FD, Jong LI, Craig VS, Shah RR, Abbott NL. Electrochemical principles for active control of liquids on submillimeter scales. Science. 1999; 283:57–60. [PubMed: 9872739]
46. Rosslee CA, Khripin C, Foley TMD, Abbott NL. Using “Prosurfactants” to enhance rates of delivery of surfactants. AlChE J. 2004; 50:708–714.
47. Meister A, Anderson ME. Glutathione. Annu Rev Biochem. 1983; 52:711–760. [PubMed: 6137189]
48. Schafer FQ, Buettner GR. Redox environment of the cell as viewed through the redox state of the glutathione disulfide/glutathione couple. Free Radic Biol Med. 2001; 30:1191–1212. [PubMed: 11368918]
49. Banhegyi G, Braun L, Csala M, Puskas F, Mandl J. Ascorbate metabolism and its regulation in animals. Free Radic Biol Med. 1997; 23:793–803. [PubMed: 9296457]
50. Guinier, A.; Fournet, G. Small angle x-ray scattering. John Wiley & Sons; New York: 1955.
51. Bellare JR, Davis HT, Scriven LE, Talmon Y. Controlled environment vitrification system - an improved sample preparation technique. J Electron Microsc Tech. 1988; 10:87–111. [PubMed: 3193246]
52. Danino D, Bernheim-Groswasser A, Talmon Y. Digital cryogenic transmission electron microscopy: An advanced tool for direct imaging of complex fluids. Colloids Surf A: Physicochem Eng Asp. 2001; 183:113–122.
53. van Gaal EVB, van Eijk R, Oosting RS, Kok RJ, Hennink WE, Crommelin DJA, Mastrobattista E. How to screen non-viral gene delivery systems in vitro? J Control Release. 201110.1016/j.jconrel.2011.05.001.
54. Vigneron JP, Oudrhiri N, Fauquet M, Vergely L, Bradley JC, Basseville M, Lehn P, Lehn JM. Guanidinium-cholesterol cationic lipids: Efficient vectors for the transfection of eukaryotic cells. Proc Natl Acad Sci U S A. 1996; 93:9682–9686. [PubMed: 8790391]
55. Gluzman Y. SV40-transformed simian cells support the replication of early SV40 mutants. Cell. 1981; 23:175–182. [PubMed: 6260373]
56. Pear WS, Nolan GP, Scott ML, Baltimore D. Production of high-titer helper-free retroviruses by transient transfection. Proc Natl Acad Sci U S A. 1993; 90:8392–8396. [PubMed: 7690960]

57. Tomlinson E, Rolland AP. Controllable gene therapy - pharmaceutics of non-viral gene delivery systems. J Control Release. 1996; 39:357–372.

58. Sakurai F, Inoue R, Nishino Y, Okuda A, Matsumoto O, Taga T, Yamashita F, Takakura Y, Hashida M. Effect of DNA/liposome mixing ratio on the physicochemical characteristics, cellular uptake and intracellular trafficking of plasmid DNA/cationic liposome complexes and subsequent gene expression. J Control Release. 2000; 66:255–269. [PubMed: 10742585]

59. Cardenas M, Dreiss CA, Nylander T, Chan CP, Cosgrove T, Lindman B. SANS study of the interactions among DNA, a cationic surfactant, and polystyrene latex particles. Langmuir. 2005; 21:3578–3583. [PubMed: 15807604]

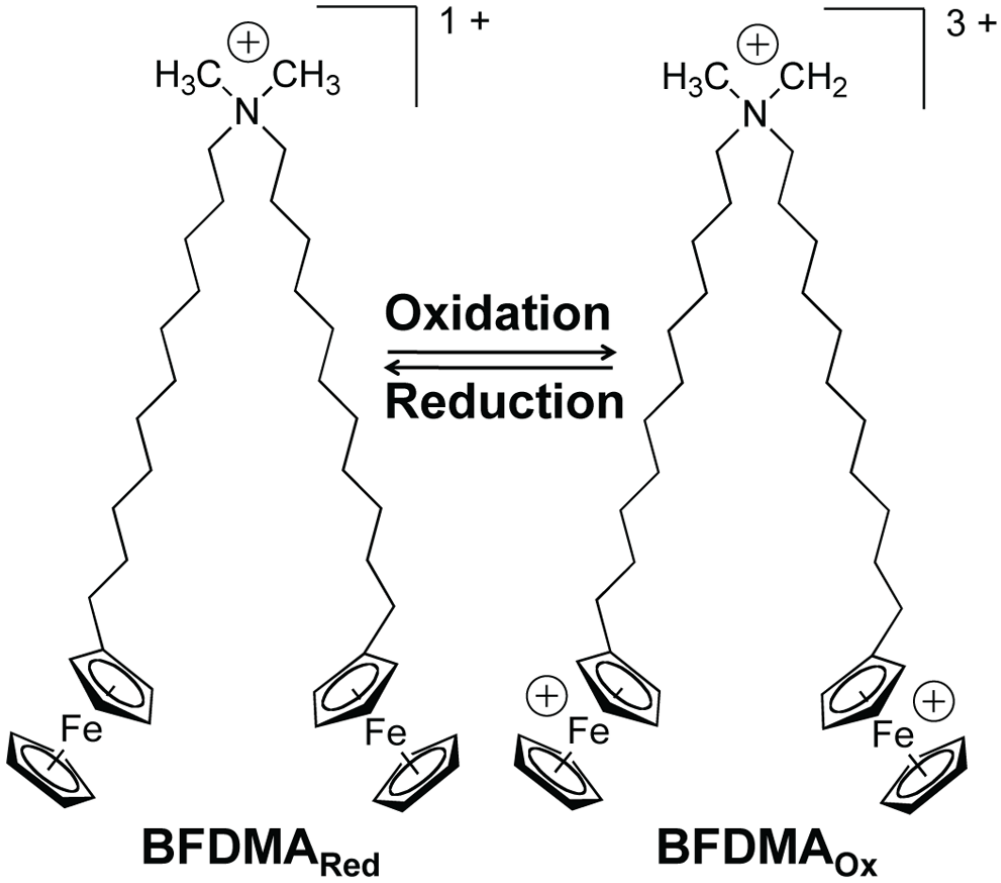

Figure 1.
Molecular structure of bis(11-ferrocenylundecyl)dimethylammonium bromide (BFDMA).

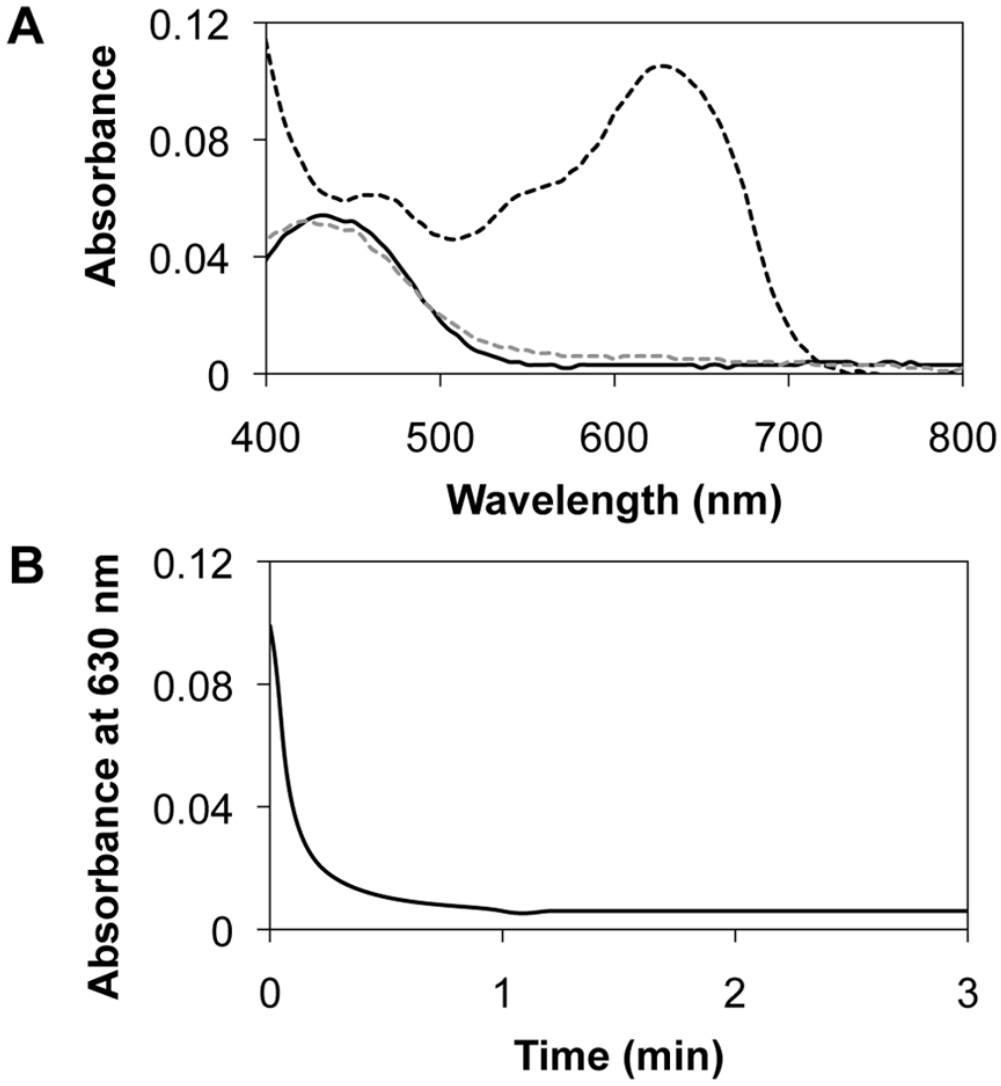

Figure 2.
(A) UV/visible absorbance spectra for solutions of lipoplexes of reduced BFDMA (black solid line), lipoplexes of oxidized BFDMA (black dashed line) or lipoplexes of oxidized BFDMA treated with AA (grey dashed line) in OptiMEM cell culture medium. (B) Decrease in absorbance maximum (630 nm) of lipoplexes of oxidized BFDMA vs time upon treatment with a 10-fold molar excess of AA in Opti-MEM cell culture

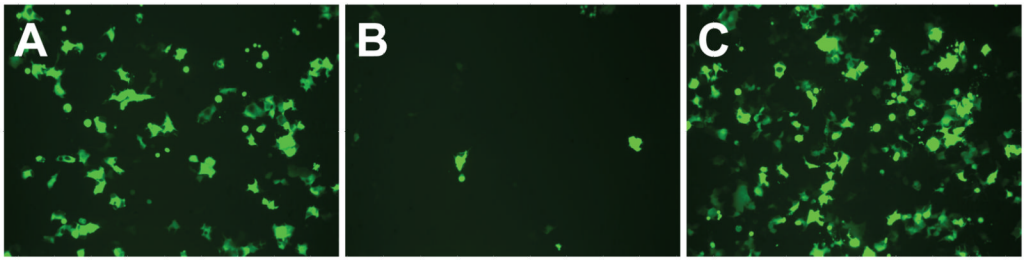

Figure 3.
Representative fluorescence micrographs (100× mag; 1194 μm × 895 μm) of confluent monolayers of COS-7 cells showing levels of EGFP expression mediated by (A) lipoplexes of reduced BFDMA, (B) lipoplexes of oxidized BFDMA or (C) lipoplexes of oxidized BFDMA treated with AA.

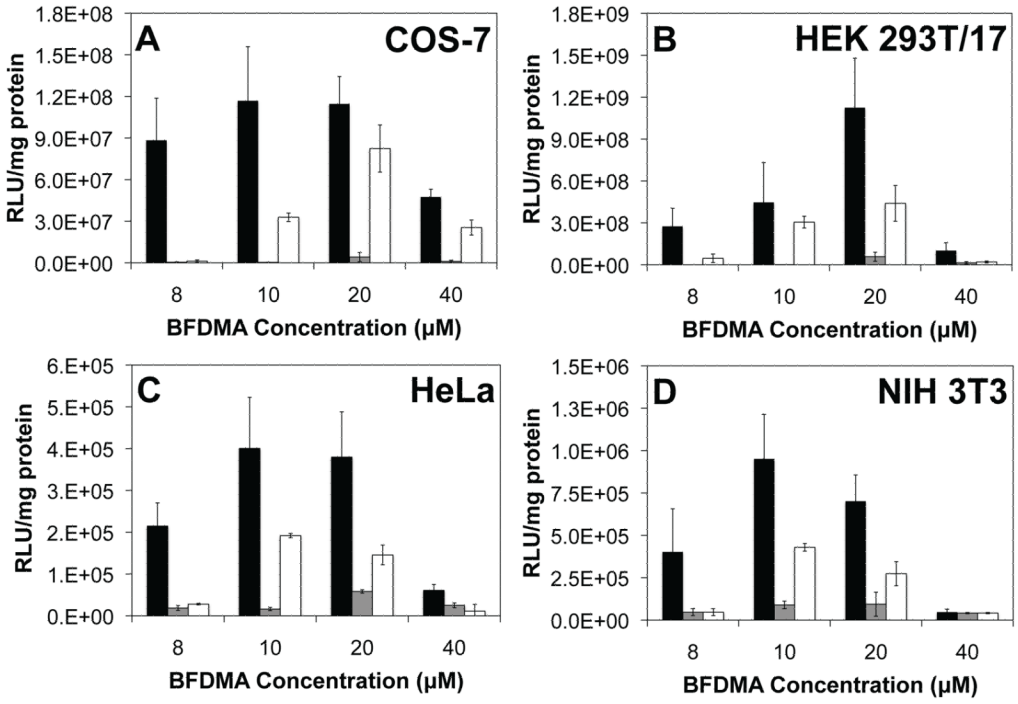

Figure 4.

Normalized luciferase expression mediated by lipoplexes of reduced BFDMA (black bars), lipoplexes of oxidized BFDMA (gray bars), or lipoplexes of oxidized BFDMA treated with AA (white bars) in (A) COS-7, (B) HEK 293T/17, (C) HeLa and (D) NIH 3T3 cell lines.

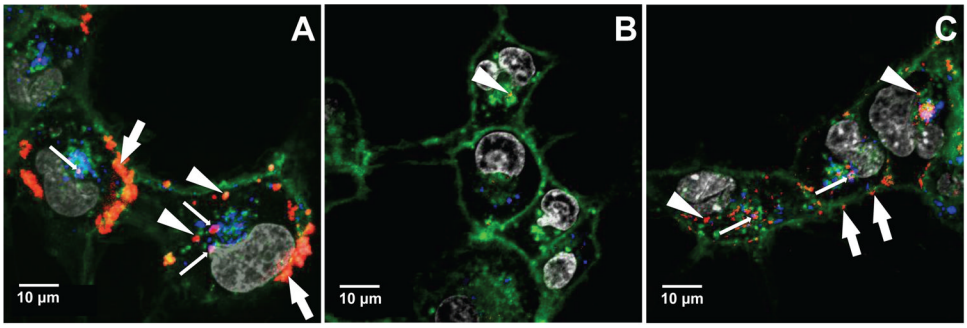

Figure 5.

Confocal fluorescence micrographs showing internalization of DNA by COS-7 cells treated with (A) lipoplexes of reduced BFDMA, (B) lipoplexes of oxidized BFDMA or (C) lipoplexes of oxidized BFDMA treated with AA. Fluorescence signals correspond to Lysotracker Red (endosome/lysosome stain; blue), WGA-Alexa Fluor 488 (membrane stain; green), Cy5 (labeled DNA; red), and Hoechst 34580 (nuclear stain; signal). Thick white arrows point to lipoplexes that appear to be associated with cell membranes, thin white arrows point to internalized lipoplexes located in endosomes and/or lysosomes, and white arrow heads point to lipoplexes that are not located in acidic endosomes or lysosomes.

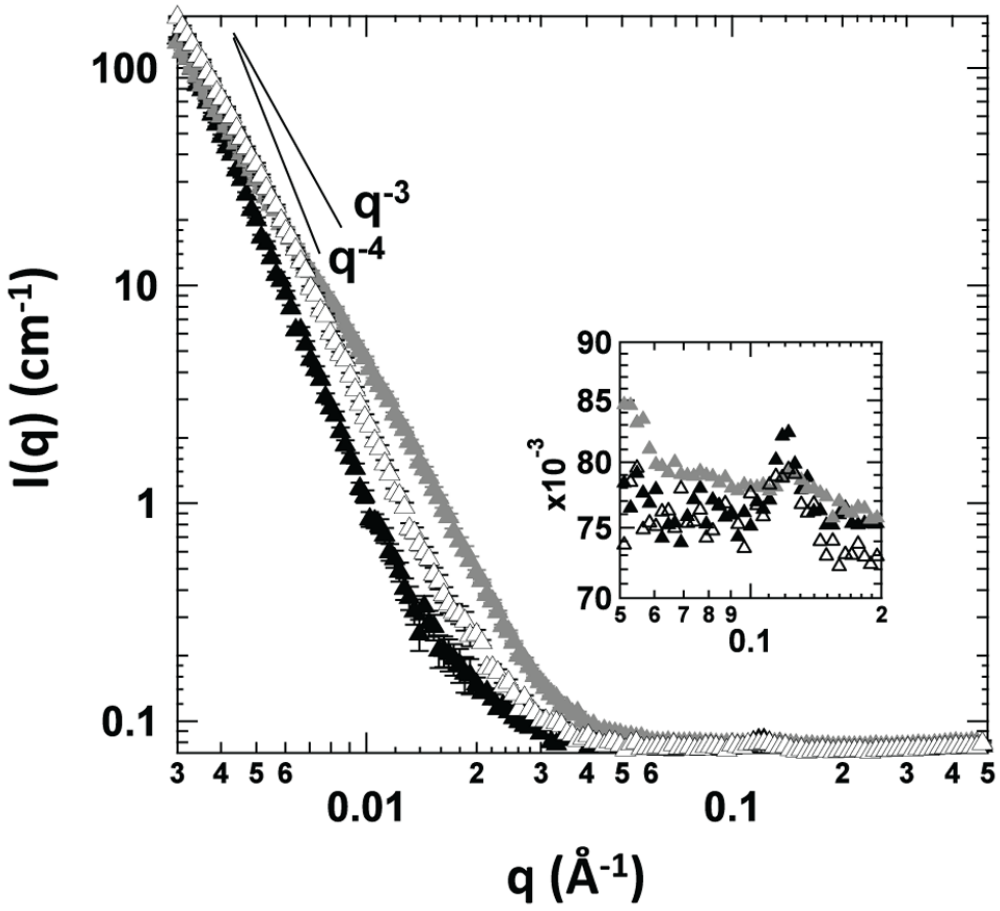

Figure 6.

SANS spectra of lipoplexes of reduced BFDMA (solid black triangles), lipoplexes of oxidized BFDMA (solid gray triangles) or lipoplexes of oxidized BFDMA treated with AA (open black triangles). The inset shows the Bragg peaks observed at 0.12 $Å^{-1}$. The data corresponding to solutions of lipoplexes of oxidized BFDMA and lipoplexes of oxidized BFDMA treated with AA were offset by a scale factor of 1.2 to facilitate direct comparison to the SANS spectrum of reduced BFDMA lipoplexes.

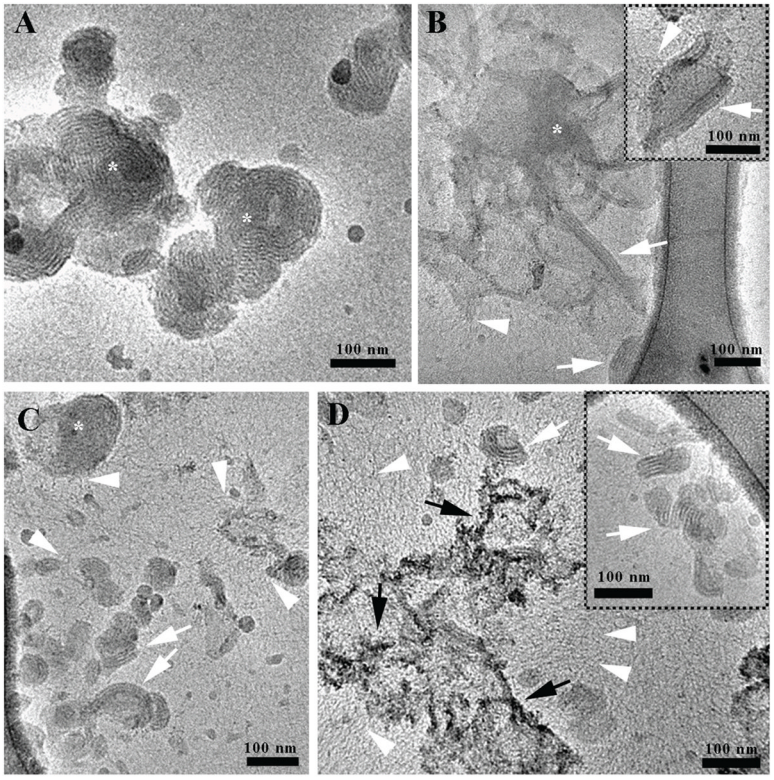

Figure 7.
Cryo-TEM images of (A) lipoplexes of reduced BFDMA (* shows onion-like lipoplexes, (B) lipoplexes of oxidized BFDMA (* shows dense amorphous aggregate), or (C,D) lipoplexes of oxidized BFDMA treated with AA in Opti-MEM. White arrows point to lamellar structures, arrowheads show DNA threadlike structures, and black arrows indicate high contrast amorphous aggregates.

Table 1

Zeta Potentials of Lipoplexes[a]

Sample	Zeta Potentials (mV)
Lipoplexes of Reduced BFDMA	−16.8 ± 1.5
Lipoplexes of Oxidized BFDMA	−33.7 ± 1.4
Lipoplexes of Oxidized BFDMA treated with AA	−20.6 ± 1.2

[a] Lipoplexes were prepared in Li_2SO_4 solution and then diluted in Opti-MEM cell culture medium so that the final concentration of BFDMA was 10 μM in all cases, and lipid/DNA charge ratios were fixed at 1.4:1 for lipoplexes of reduced BFDMA and 4.2:1 for lipoplexes of oxidized BFDMA. Lipoplexes of oxidized BFDMA were treated with 10-fold molar excess of AA following their dilution into Opti-MEM cell culture medium.